Nat. Hazards Earth Syst. Sci. Discuss., 3, 4919–4935, 2015
www.nat-hazards-earth-syst-sci-discuss.net/3/4919/2015/
doi:10.5194/nhessd-3-4919-2015

Natural Hazards and Earth System Sciences Discussions
Open Access

A numerical study of the early stages of a tropical cyclogenesis in relation to the MJO

J. Guerbette[1,2], M. Plu[1,2], C. Barthe[1], and J.-F. Mahfouf[2]

[1]Laboratoire de l'Atmosphère et des Cyclones, Unité Mixte CNRS/Météo-France/Université de La Réunion, La Réunion, France
[2]CNRM-GAME, Météo-France/CNRS, Toulouse, France

Received: 1 July 2015 – Accepted: 2 August 2015 – Published: 19 August 2015

Correspondence to: J. Guerbette (jeremy.guerbette@meteo.fr)

Published by Copernicus Publications on behalf of the European Geosciences Union.

A numerical study of the early stages of a tropical cyclogenesis in relation to the MJO

J. Guerbette et al.

Abstract

The role of an active phase of the Madden–Julian Oscillation (MJO) on the evolution of a mesoscale convective systems (MCS) leading to a tropical depression is investigated in the South-West Indian Ocean during the Dynamics of the Madden–Julian Oscillation (DYNAMO) field experiment, with a numerical limited-area atmospheric model. A mesoscale vortex is followed in the low-troposphere from the initiation of the active MJO phase. It is shown that the interaction of the vortex with the Equatorial jet associated with the MJO plays an important role on the vortex development. As the vortex encounters the southern part of the low-level jet, it undergoes intensification that is explained by the barotropic conversion of kinetic energy from the low-level jet to the vortex.

1 Introduction

Tropical cyclogenesis remains a worldwide scientific challenge that is important for forecasting applications on many time ranges: for daily forecasts, seasonal forecasts and climate projections. Necessary environmental ingredients for cyclogenesis have been known since the work of Gray (1968). Under such conditions, some of the mesoscale convective systems (MCS) that evolve for several days may develop, interact, or merge (Ritchie and Holland, 1997) and eventually lead to cyclone formation (Simpson et al., 1997). The sufficient conditions for cyclogenesis are still an open scientific question, and they should be looked for in the synoptic-scale environment and in the life cycle and structure of the MCS (Kerns and Chen, 2013).

Many studies have been arguing that the early stage of cyclone formation is stochastic to some extent, but the large-scale environment of the MCS may also determine the organisation of convection (Ooyama, 1982; Simpson et al., 1997; Tory et al., 2007) and favour cyclogenesis or not. Studying the development of MCS in relation to their environment is thus critical to understand and to forecast cyclogenesis and also to assess

NHESSD

3, 4919–4935, 2015

the predictability of cyclogenesis. For instance, in the North Atlantic ocean, easterly waves over North Africa play a critical role on the development of MCS and on cyclogenesis by vortex initiation (Sall et al., 2006; Arnault and Roux, 2010). In other ocean basins, synoptic-scale environments are different and their interaction with MCS should take other paths.

The South-West Indian Ocean is the third most active cyclone basin of the world, with more than 10 tropical storms on average per year (Neumann, 1993). However few studies have addressed the role of environmental conditions on cyclogenesis in this basin. Bessafi and Wheeler (2006) studied the link between large-scale equatorial waves and cyclogenesis. They revealed that active phases of the Madden–Julian Oscillation (MJO, Madden and Julian, 1994) are favourable to cyclogenesis. The recent statistical study of Duvel (2015) emphasized that the initiation of cyclones during a MJO active phase is favoured by unstable meridional shear. The present study aims at studying the early stages of a cyclogenesis in the South-West Indian Ocean during an active phase of MJO and at identifying the role of the synoptic environment on a MCS formation that leads later to a tropical cyclone. To this end, a particular MCS development observed during the Dynamics of the Madden–Julian Oscillation (DYNAMO) field experiment is considered, and is studied with a numerical limited-area atmospheric model. The boundary conditions of the simulation benefit from additional atmospheric observations made during DYNAMO.

The article is organized as follows. The case study and the numerical model are presented in Sect. 2. Section 3 details the evolution of the simulated MCS and of its environment, before undertaking an energetic budget analysis of the interaction of the MCS with its environment in Sect. 4. The main findings are summarized in a brief conclusion.

NHESSD
3, 4919–4935, 2015

2 The case study and numerical simulations

The tropical cyclone Regional Specialized Meteorological Centre (RSMC) of La Réunion monitored the second tropical depression of the cyclone season from the 3 to the 14 December 2011. The environmental conditions of the pre-formation were typical of cyclogenesis of the early season in the South-West Indian Ocean. Infrared images from geostationary satellite MeteoSat 7 (not shown) reveal that large-scale convection developed from the 21 November around the Equator during the initiation of an MJO active phase in the Indian Ocean (MJO analysis available at http://www.bom.gov.au/climate/mjo/graphics/rmm.74toRealtime.txt). This large-scale convective event lasted several days during the DYNAMO experiment (Zuluaga and Houze, 2013). Dedicated observations during the experiment were collected in near-real time and assimilated in numerical weather prediction models. As a consequence, the operational Integrated Forecast System (IFS) from the European Centre for Medium-Range Meteorological Forecasts (ECMWF) assimilated supplementary radiosonde measurements at four stations (the corners of the red polygon on Fig. 1) at least four times per day. Images from Meteosat 7 show that the cyclone separates from the large-scale convection environment from the 30 November, around latitude 10° S and longitude 75° E. In order to study the role of the MJO active phase on the formation of the cyclone, a simulation was run with the Meso-NH numerical model (Lafore et al., 1998) between 20 and 30 November 2011, with initial and lateral boundary conditions taken from ECMWF operational analyses.

The case study was simulated with a version of Meso-NH having a horizontal grid spacing of 8 km. The vertical grid has 70 levels up to 27 km with spacing from 40 m (bottom) up to 600 m (top). A sponge layer was applied from 23 to 27 km in order to dampen the upward-propagating gravity waves generated by convection. The domain covered the DYNAMO region with an area of about 2400 km × 1600 km as shown in Fig. 1. The time step for advection was 16 s. The physical parametrizations included the representation of turbulence following the turbulent energy closure of Bougeault and Lacarrère

NHESSD
3, 4919–4935, 2015

(1989). Sub-grid moist convection was described with a mass-flux scheme (Bechtold et al., 2001). Resolved clouds evolved following the mixed-phase microphysical description of Pinty and Jabouille (1998) including a subgrid cloudiness diagnostic of Chaboureau and Bechtold (2005). The radiative transfer processes were accounted for with the ECMWF longwave and shortwave schemes (Gregory et al., 2000). The sea-surface temperature is imposed from ECMWF analyses and turbulent surface fluxes over oceans are diagnosed using the ECUME scheme (Belamari and Pirani, 2007).

In order to locate the origin of the depression, vortex tracking has been performed on the Meso-NH outputs every 3 h at 850 hPa from the 3 December backward in time. On the 3 December 18:00 UTC, the vortex centre is given by RSMC La Réunion best-track. At previous times, the vortex centre is identified as the closest vorticity relative minimum which value is below $-0.5 \times 10^{-3}\,s^{-1}$ (the vorticity in a cyclone is negative in the Southern Hemisphere). This procedure that has been applied recursively allows to follow the vortex back until the 21 November (Fig. 1), corresponding to the MJO initiation. The vortex track moves towards the North-West and then to the North-East until the 23 November. At this time, the vortex enters rapidly the DYNAMO domain (red box in Fig. 1) by its west side. From 24 to 29 November, the vortex stays in the DYNAMO domain with a slow displacement. On the 30 November, the vortex goes out of the DYNAMO domain toward the south before being monitored by RSMC La Réunion. During its lifetime, the vortex is associated with various phases of intense convection, that are captured by the Meso-NH simulation. Meteosat infrared images confirm the existence of several isolated MCS in the domain of interest.

A validation of the simulated evolution of the vortex may be done using surface ocean winds from the OSCAT scatterometer. The 10 m wind simulated by Meso-NH and observed from OSCAT data (Purna et al., 2014) are compared in Fig. 2. Meso-NH produces a maximum 10 m wind speed of $26\,m\,s^{-1}$ centred at (3° S; 76° E) the 28 November 2011 at 18:00 UTC (Fig. 2a). At that particular time, the OSCAT scatterometer measured a maximum surface wind speed of $24\,m\,s^{-1}$ centred at (6° S; 76° E) (Fig. 2b). This confirms that the intensity is well simulated even if the vortex centre is

NHESSD
3, 4919–4935, 2015

located ∼ 300 km too north in the simulation. Since no OSCAT swath is available before this time over the vortex centre, the validation of the whole predicted track between the 20 and 29 November is not possible.

3 Evolution of the MCS and of its environment in the simulation

From the Meso-NH numerical simulation, the evolution of the vortex strength can be described. Figure 3 shows the evolution of the maximum simulated vorticity between the 23 November and the 30 November at 4 levels: 850, 700, 500 and 200 hPa. The vortex centre is known from the tracking at 850 hPa described in Sect. 2. Upper level vorticity values are obtained at the locations straight up to the vortex centre at 850 hPa, which are close to the vortex centres at the upper levels when they exist.

The strength of the vortex at 850 hPa evolves with time, with successive phases of intensification and weakening. The values of vorticity at 700 hPa are close to and well correlated to the ones at 850 hPa, revealing that the vortex structure remains at least as up as 700 hPa during all the period. On the contrary, vorticity values at 500 and 200 hPa are not well correlated to the vortex strength at lower levels and they remain generally weaker. Three phases of vortex intensification at low levels have been identified, revealing different behaviours across the vertical levels:

- a phase of moderate intensification that begins on the 23, at 850, 700 hPa and to a less extent at 500 hPa, followed by a rapid increase at all levels on the 24, around 12:00 UTC, which is consistent with a convective burst of the MCS,
- a short phase of moderate intensification around the 25, that is present up to 700 hPa, and also at 500 hPa to some extent,
- a long phase of slow intensification at all levels from the 27 until the 29.

Keeping in view that convection and diabatic processes could be important in the vortex intensification, the role of the environment on the evolution of the MCS intensity is

NHESSD
3, 4919–4935, 2015

investigated. An active phase of the MJO is associated with a large-scale easterly jet in the low-troposphere that propagates slowly towards the East (Madden and Julian, 1994). The MJO remains generally active in the Indian Ocean during a time-period of 10 days. It is thus relevant to investigate the role of this low-level jet on the vortex intensification. To conduct such an analysis, each model variable ε at time t is split into an environment value plus an anomaly part:

$$\varepsilon(t) = \overline{\varepsilon}(t) + \varepsilon'(t) \tag{1}$$

where $\varepsilon(t)$ is an average-state solution of the model computed over 10 days centred at instant t and ε' is the residual perturbation field. A 10 day low-pass filter has been chosen for the environment in order to have the best representation of the equatorial jet structure associated with the MJO. Figure 4 shows the extension of the low-frequency jet at 850 hPa, showing the most intense horizontal gradients of the jet, where interaction may be favoured, around the latitudes 4 to 6° S. The MCS vortex evolves around these latitudes during two periods (Fig. 1): the first one during the 24 November, and the second one during the 27th. It is worth noting that these periods also correspond to two of the phases of intensification identified in Fig. 3. Figure 4 focuses on the evolution of the vortex with the jet during the first period of interaction, as it evolves southward out of the low-level jet, in the area where the horizontal wind gradient is the strongest. However, further diagnostics are needed to understand the interaction of the MCS with the jet.

4 Energetics of the low-level cyclone

The jet–vortex interactions are examined more precisely through an energy budget analysis. Although initially developed for the large-scale circulation under the adiabatic assumption, the Lorenz (1955) cycle proved to be useful to understand environment-anomaly interactions in a large range of contexts (Arbogast, 2004). It has been indeed

NHESSD
3, 4919–4935, 2015

applied to study the intensification of African Easterly Waves and the possible subsequent cyclogenesis over North Atlantic in relation to their environment (Norquist et al., 1997; Hsieh and Cook, 2007). For a similar purpose, Arnault and Roux (2010) used such an approach on the outputs of a mesoscale numerical simulation.

The energetics analysis decomposes atmospheric fields into an anomaly and an environment components as described in Sect. 3. We focus on the diagnosis of kinetic energy within a 2° × 2° box (Fig. 4) around the MCS vortex centre at 850 hPa. The evolution equation of the kinetic energy of the perturbation K' can be written as:

$$\frac{\mathrm{d}K'}{\mathrm{d}t} = \frac{1}{2}\frac{\mathrm{d}u'^2}{\mathrm{d}t} = C_\mathrm{B} + C_\mathrm{I} + A_x \qquad (2)$$

where

$$C_\mathrm{B} = -K'\left(\frac{\partial \overline{u}}{\partial x} + \frac{\partial \overline{v}}{\partial y}\right) - \left(\frac{u'^2 - v'^2}{2}\right)\left(\frac{\partial \overline{u}}{\partial x} - \frac{\partial \overline{v}}{\partial y}\right) - u'v'\left(\frac{\partial \overline{u}}{\partial y} + \frac{\partial \overline{v}}{\partial x}\right) \qquad (3)$$

is the barotropic conversion (Lorenz, 1955), which represents the transfer of kinetic energy from the environment (i.e. the large-scale jet) towards the kinetic energy of the perturbation (i.e. the box around the vortex at 850 hPa), and

$$C_\mathrm{I} = -\frac{R}{T}T'\omega' \qquad (4)$$

is the internal conversion, which represents the transfer of potential energy of the perturbation towards kinetic energy. The term A_x is not computed here: it accounts for geopotential fluxes, diabatic terms and fluxes at the box boundaries (Arbogast, 2004). Since it can reach quite large values, it will not be possible to close the budget.

To understand the vortex energetics at 850 hPa, the vorticity and various terms of Eq. (2) (except A_x) are examined at that level (Fig. 5). The time periods when the vortex encounters the southern part of the jet, on the 24 and on the 27 November, are highlighted (shaded grey areas in Fig. 5). These time periods of vortex intensification are

NHESSD
3, 4919–4935, 2015

consistently preceded (roughly by a 6 h time lag) with positive tendencies of the perturbation kinetic energy. During the first period (on the 24), the contribution of barotropic conversion to the increase of kinetic energy reaches high positive values, which is also the case for internal conversions. These conversions get back to negative values afterwards. Barotropic conversion reaches again sustained positive values on the 27, when again the vortex encounters the jet and intensifies. Both phases are associated to a transfer of kinetic energy from the jet to the vortex, showing that the large-scale jet plays a significant role in enhancing vorticity through barotropic conversion (Arbogast, 2004). After the 27, the slow vortex intensification is associated with sustained positive barotropic and internal conversions. The negative kinetic energy tendency cannot be explained by these conversion terms and could be due to adiabatic terms and energy redistribution along the vertical.

It is relevant also to note that during the short period of intensification of the 25 November, as the vortex remains far away from the jet, barotropic and internal conversions have low values.

5 Conclusions

Tropical cyclones are important weather hazards and their genesis needs to be better understood, in order to improve their prediction. The present study aims at describing the life cycle of a MCS during an active phase of the MJO, leading to a cyclogenesis in the South-West Indian Ocean. A numerical simulation of the atmosphere was run with the limited-area Meso-NH model and the environmental influence on the vortex growth has been examined in details using energetic diagnostics. The main conclusions are:

- the vortex undergoes a complex evolution, with phases of intensification and vertical development, followed by phases of stagnation;

- the main phases of intensification occur when the vortex approaches (and interacts with) the large-scale Equatorial jet typical of the MJO structure;

NHESSD
3, 4919–4935, 2015

– the large-scale jet plays a critical role on the vortex intensification through barotropic processes in the low troposphere.

This study emphasizes the specific role that the Equatorial jet associated with an active phase of the MJO has on the early stages of a cyclogenesis. This is an important result for the predictability of cyclogenesis since it is very likely that such a large-scale jet may be more predictable than small-scale unorganized convection.

As a perspective, it would be interesting to assess whether the dynamical processes shown for this particular MCS also apply to cyclogenesis situations in the South-West Indian Ocean. For example, the tropical cyclones Anja in 2009 and Benilde (Duvel, 2015) in 2011 seem to have undergone a similar evolution during their early stages.

Acknowledgements. Computer resources were allocated by GENCI (project 6660).

References

Arbogast, P.: Frontal-wave development by interaction between a front and a cyclone: application to FASTEX IOP 17, Q. J. Roy. Meteor. Soc., 130, 1675–1696, 2004.

Arnault, J. and Roux, F.: Case study of a developing African easterly wave during NAMMA: an energetic point of view, J. Atmos. Sci., 66, 2991–3020, 2010.

Bechtold, P., Bazile, E., Guichard, F., Mascart, P., and Richard, E.: A mass flux convection scheme for regional and global models, Q. J. Roy. Meteor. Soc., 127, 869–886, 2001.

Belamari, S. and Pirani, A.: Validation of the optimal heat and momentum fluxes using the ORCA-2-LIM global ocean-ice model, Marine Environment and Security for the European Area Integrated Project (MERSEA IP), deliverable D4.1.3, 88 p., 2007.

Bessafi, M. and Wheeler, M. C.: Modulation of South Indian Ocean tropical cyclones by the Madden–Julian oscillation and convectively coupled equatorial waves, Mon. Weather Rev., 134, 638–656, 2006.

Bougeault, P. and Lacarrère, P.: Parametrization of orography-induced turbulence in a mesoscale model, Mon. Weather Rev., 117, 1872–1890, 1989.

Chaboureau, J. P. and Bechtold, P.: Statistical representation of clouds in a regional model and the impact on the diurnal cycle of convection during Tropical Convection, Cirrus and Nitrogen Oxides (TROCCINOX), J. Geophys. Res., 110, D17103, doi:10.1029/2004JD005645, 2005.
Duvel, J- P.: Initiation and intensification of tropical depressions over the Southern Indian Ocean: influence of the MJ O, Mon. Weather Rev., 143, 2170–2191, 2015.
Gray, M. W.: Global view of the origin of tropical disturbances and storms, Mon. Weather Rev., 96, 669–700, 1968.
Gregory, D., Morcrette, J. J., Jakob, C., Beljaars, A. C. M., and Stockdale, T.: Revision of convection, radiation and cloud schemes in the ECMWF Integrated Forecasting System, Q. J. Roy. Meteor. Soc., 126, 1685–1710, doi:10.1256/smsqj.56607, 2000.
Hsieh, J.-S. and Cook, K. H.: A study of the energetics of African easterly waves using a regional climate model, J. Atmos. Sci., 64, 421–440, 2007.
Kerns, B. W and Shuyi, S. C.: Cloud Clusters and Tropical Cyclogenesis: developing and non-developing systems and their large-scale environment, Mon. Weather Rev., 141, 192–210, 2013.
Lafore, J. P., Stein, J., Asencio, N., Bougeault, P., Ducrocq, V., Duron, J., Fischer, C., Héreil, P., Mascart, P., Masson, V., Pinty, J. P., Redelsperger, J. L., Richard, E., and Vilà-Guerau de Arellano, J.: The Meso-NH Atmospheric Simulation System. Part I: adiabatic formulation and control simulations, Ann. Geophys., 16, 90–109, doi:10.1007/s00585-997-0090-6, 1998.
Lorenz, E. N.: Available potential energy and the maintenance of the general circulation, Tellus, 7, 157–167, 1955.
Madden, R. and Julian, P. R.: Observations of the 40–50 day tropical oscillation – a review, Mon. Weather Rev., 122, 814–837, 1994.
Neumann, C. J.: Global guidance to tropical cyclone forecasting, Chapter 1: global overview, WMO Tropical Cyclone Program, Report TCP-31. 43 p., 1993.
Norquist, D. C., Recker, E. E., and Reed, R. J.: The energetics of African wave disturbances as observed during phase III of GATE, Mon. Weather Rev., 105, 334–342, 1977.
Ooyama, K. V.: Conceptual evolution of the theory and modelling of the tropical cyclone, J. Meteorol. Soc. Jpn., 60, 369–380, 1982.
Pinty, J. P. and Jabouille, P.: A mixed-phase cloud parametrization for use in mesoscale non-hydrostatic model: simulations of a squall line and of orographic precipitations, Proceedings of the AMS Conference on Cloud Physics, Everett, WA, USA, August 1999, American Meteorological Society, Boston, 217–220, 1998.

NHESSD
3, 4919–4935, 2015

Purna Chand, C., Rao, M. V., Ramana, I.V, Ali, M. M., Patoux, J., and Bourassa, M. A.: Estimation of sea level pressure fields during Cyclone Nilam from Oceansat-2 scatterometer winds, Atmos. Sci. Letter, 15, 65–71, doi:10.1002/asl2.473, 2014.
Ritchie, E. and Holland, G. J.: Scale interaction during the formation of typhoon Irving, Mon. Weather Rev., 125, 1377–1396, 1997.
Sall, S. M., Sauvageot, H., Gaye, A., Viltard, A., and de Félice, P.: A cyclogenesis index for tropical Atlantic off the African coast, Atmos. Res., 79, 123–147, 2006.
Simpson, J, Ritchie, E., Holland, G. J., Halverson, J., and Stewart, S.: Mesoscale interactions in tropical cyclone genesis, Mon. Weather Rev., 125, 2643–2661, 1997.
Tory, K. J., Davidson, N. E., and Montgomery, M. T.: Prediction and diagnosis of tropical cyclone formation in an NWP system, Part III: Diagnosis of developing and nondeveloping storms, J. Atmos. Sci., 64, 3195–3213, 2007.
Zuluaga, M. D. and Houze, R. A.: Evolution of the population of precipitating convective systems over the equatorial Indian Ocean in active phases of the Madden–Julian oscillation, J. Atmos. Sci., 70, 2713–2725, 2013.

NHESSD
3, 4919–4935, 2015

A numerical study of the early stages of a tropical cyclogenesis in relation to the MJO

J. Guerbette et al.

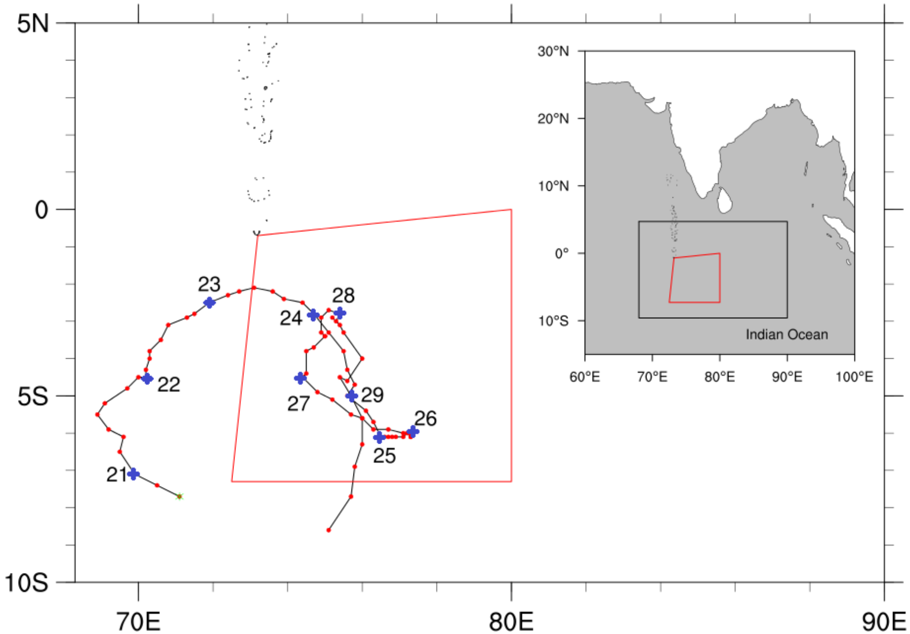

Figure 1. Evolution of the position of the vortex centre of a MCS simulated by Meso-NH from 21 to 29 November 2011 every 3 h (red dots linked by the black curve). The corners of the red quadrangle are the stations from which supplementary radiosondes were launched during the DYNAMO experiment. The domain of the Meso-NH simulation is displayed as a black rectangle in the upper-right panel.

NHESSD
3, 4919–4935, 2015

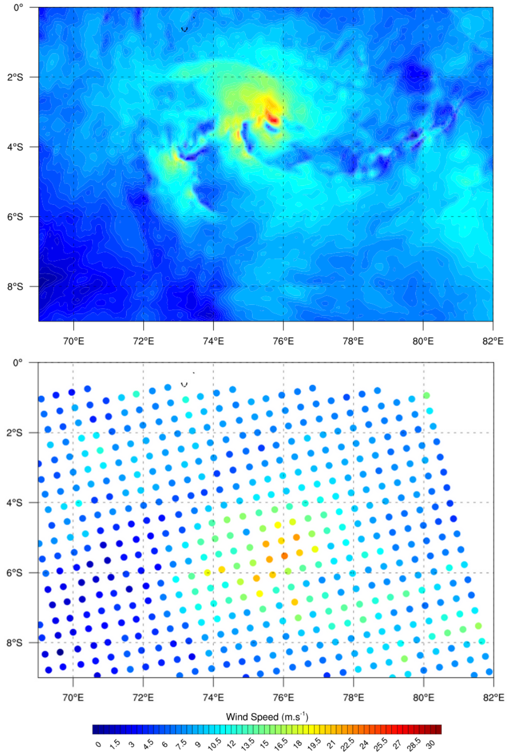

Figure 2. 10 m wind speed simulated by meso-NH (top) and observed by scatterometer OSCAT (bottom) on the 28 November 2011 at 18:00 UTC.

NHESSD
3, 4919–4935, 2015

A numerical study of the early stages of a tropical cyclogenesis in relation to the MJO

J. Guerbette et al.

Title Page
Abstract Introduction
Conclusions References
Tables Figures
◂ ▸
Back Close
Full Screen / Esc
Printer-friendly Version
Interactive Discussion

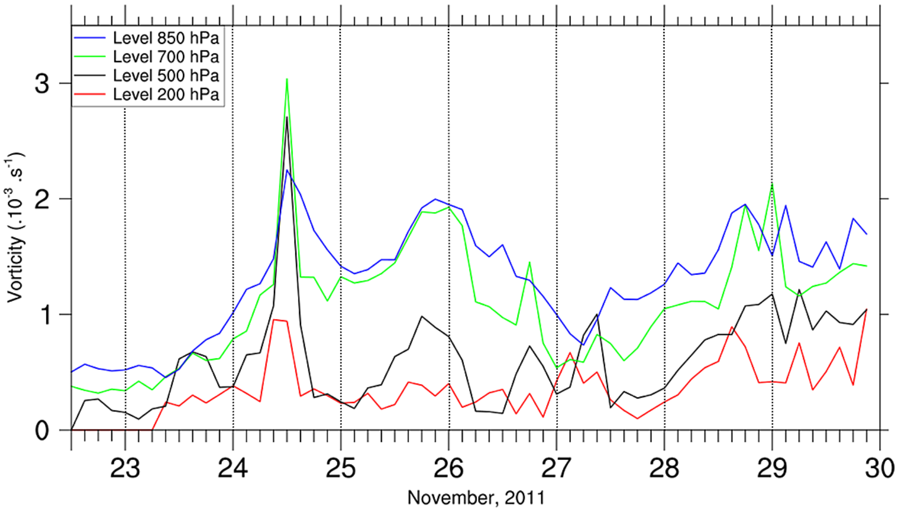

Figure 3. Evolution of the maximum of the absolute value of vorticity of the vortex identified in Fig. 1 at 4 levels: 850, 700, 500 and 200 hPa between the 23 November at 12:00 UTC and the 30 November 2011 at 00:00 UTC.

NHESSD
3, 4919–4935, 2015

A numerical study of the early stages of a tropical cyclogenesis in relation to the MJO

J. Guerbette et al.

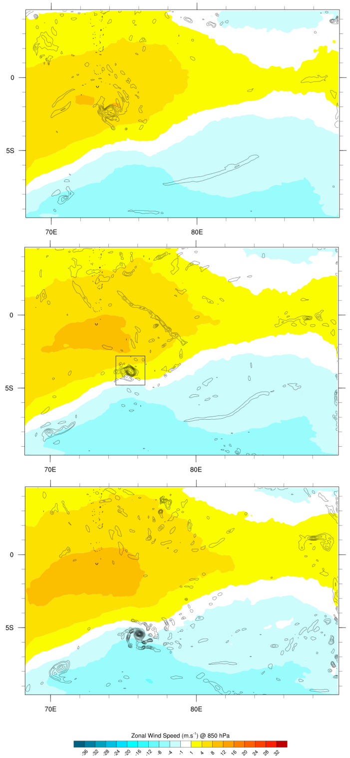

Figure 4. 10 day mean of zonal wind (colors; $> 0\,\mathrm{m\,s^{-1}}$: toward east) and relative vorticity anomaly (black contours, isolines $1.10^{-4}\,\mathrm{s^{-1}}$, shown only below $-1.10^{-4}\,\mathrm{s^{-1}}$) at 850 hPa on 23 November at 15:00 UTC (top), 24 November at 03:00 UTC (middle) and 24 November at 15:00 UTC (bottom) simulated by the Meso-NH model. The black square ($2^\circ \times 2^\circ$) is the one used for energetic budget; it is located at each instant around the vortex centre.

NHESSD
3, 4919–4935, 2015

Title Page
Abstract | Introduction
Conclusions | References
Tables | Figures
◀| |▶
◀ ▶
Back | Close
Full Screen / Esc
Printer-friendly Version
Interactive Discussion

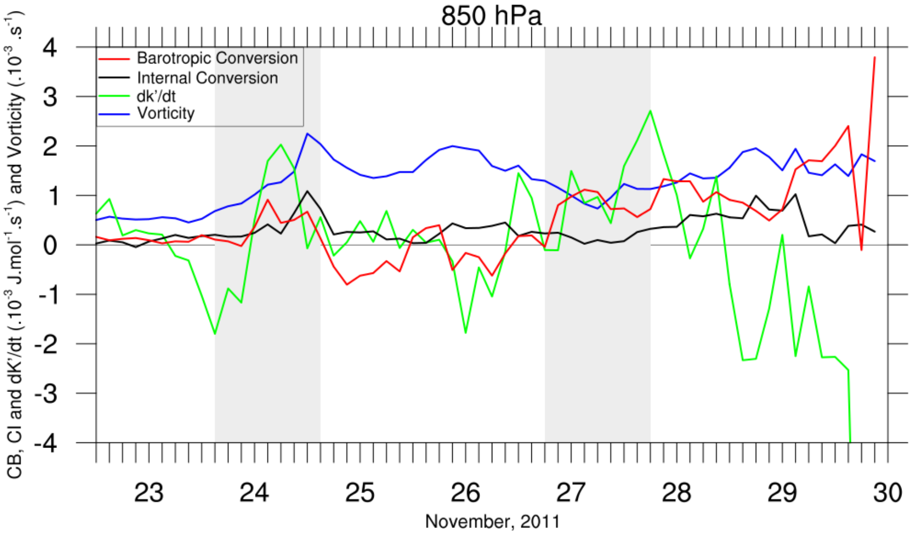

Figure 5. Time evolution of absolute value of vorticity (blue line), tendency of the kinetic energy of the perturbation K' (green line), internal (black line) and barotropic conversion (red line) of the perturbation in a 2°-side box centred on the vortex centre at 850 hPa during 7 days in November 2011. The grey boxes represent the periods when the vortex is embedded in the southern part of the large-scale jet.

NHESSD
3, 4919–4935, 2015